PROTEINS
STRUCTURE ■ FUNCTION ■ BIOINFORMATICS

Apo-parvalbumin as an intrinsically disordered protein

Sergei E. Permyakov,[1] Anush G. Bakunts,[1] Alexander I. Denesyuk,[1,2] Ekaterina L. Knyazeva,[1] Vladimir N. Uversky,[1,3]* and Eugene A. Permyakov[1]*

[1] Institute for Biological Instrumentation of the Russian Academy of Sciences, Pushchino, Moscow Region 142290, Russia
[2] Department of Biochemistry and Pharmacy, Åbo Akademi University, Artillerigatan 6A, FI-20520 Turku, Finland
[3] Institute of Intrinsically Disordered Proteins, Center for Computational Biology and Informatics, Department of Biochemistry and Molecular Biology, Indiana University School of Medicine, Indianapolis, Indiana 46202

ABSTRACT

Recently defined family of intrinsically disordered proteins (IDP) includes proteins lacking rigid tertiary structure meanwhile fulfilling essential biological functions. Here we show that apo-state of pike parvalbumin (α- and β-isoforms, pI 5.0 and 4.2, respectively) belongs to the family of IDP, which is in accord with theoretical predictions. Parvalbumin (PA) is a 12-kDa calcium-binding protein involved into regulation of relaxation of fast muscles. Differential scanning calorimetry measurements of metal-depleted form of PA revealed the absence of any thermally induced transitions with measurable denaturation enthalpy along with elevated specific heat capacity, implying the lack of rigid tertiary structure and exposure of hydrophobic protein groups to the solvent. Calcium removal from the PAs causes more than 10-fold increase in fluorescence intensity of hydrophobic probe bis-ANS and is accompanied by a decrease in α-helical content and a marked increase in mobility of aromatic residues environment, as judged by circular dichroism spectroscopy (CD). Guanidinium chloride-induced unfolding of the apo-parvalbumins monitored by CD showed the lack of fixed tertiary structure. Theoretical estimation of energetics of the charge–charge interactions in the PAs indicated their pronounced destabilization upon calcium removal, which is in line with sequence-based predictions of disordered protein chain regions. Far-UV CD studies of apo-α-PA revealed hallmarks of cold denaturation of the protein at temperatures below 20°C. Moreover, a cooperative thermal denaturation transition with mid-temperature at 10–15°C is revealed by near-UV CD for both PAs. The absence of detectable enthalpy change in this temperature region suggests continuous nature of the transition. Overall, the theoretical and experimental data obtained show that PA in apo-state is essentially disordered nevertheless demonstrates complex denaturation behavior. The native rigid tertiary structure of PA is attained upon association of one (α-PA) or two (β-PA) calcium ions per protein molecule, as follows from calorimetric and calcium titration data.

Proteins 2008; 72:822–836.

Key words: *protein intrinsic disorder; thermodynamics; phase transition; continuous transition; cold denaturation; intermediate; metal binding.*

INTRODUCTION

Many functional proteins or protein regions are intrinsically disordered; that is, they exist as dynamic structural ensembles without fixed tertiary structure.[1–10] Disordered proteins and regions have been grouped into at least two broad structural classes—compact (molten globule-like) and extended (coil-like and premolten globule-like, so called natively unfolded proteins).[4,7–9,11,12] It has been pointed out that amino acid sequences encoding the disordered proteins or regions are significantly different from those, which are characteristic for the ordered proteins, on the basis of local amino acid composition, flexibility, hydropathy, charge, coordination number, and several other factors.[3,4] Some of these features were utilized to develop various disorder predictors (systemized at www.disprot.org).

Application of the disorder predictors to different proteomes revealed that disorder increases from bacteria to archaea to eukaryota with over a half of the eukaryotic proteins containing predicted disordered regions.[4,13–15] Importantly, the majority of known signal transduction proteins are predicted to contain significant regions of

Abbreviations: bis-ANS, 4,4′-dianilino-1,1′-binaphthyl-5,5′-disulfonic acid; CD, circular dichroism; DSC, differential scanning calorimetry; DTPA, (carboxymethylimino)bis (ethylenenitrilo)tetraacetic acid; EDTA, ethylenediaminetetraacetic acid; EGTA, ethylene glycol-bis(β-aminoethyl ether)-N,N,N′,N′-tetraacetic acid; FDPB, finite difference Poisson-Boltzmann method of calculation of electrostatic potentials; GdmCl, guanidinium chloride; HEPES, N-(2-hydroxyethyl)piperazine-N′-(2-ethanesulfonic acid); PA, parvalbumin; α-PA, α isoform of parvalbumin; β-PA, β isoform of parvalbumin; PONDR, predictors of natural disordered region; SDS-PAGE, sodium dodecyl sulfate polyacrylamide gel electrophoresis.

Grant sponsors: Program of the Russian Academy of Sciences «Molecular and Cellular Biology»; «Russian Science Support Foundation»; Foundation of Åbo Akademi; Sigrid Jusélius Foundation.
*Correspondence to: Eugene A. Permyakov, Institute for Biological Instrumentation of the Russian Academy of Sciences, Pushchino, Moscow region, 142290 Russia. E-mail: permyakov@ibp-ran.ru; or Vladimir N. Uversky, Department of Biochemistry and Molecular Biology, Indiana University School of Medicine, 635 Barnhill Drive, MS no. 4021, Indianapolis, IN 46202. E-mail: vuversky@iupui.edu
Received 22 October 2007; Revised 19 December 2007; Accepted 27 December 2007
Published online 7 February 2008 in Wiley InterScience (www.interscience.wiley.com). DOI: 10.1002/prot.21974

disorder.[16] Despite lacking any stable tertiary structure, intrinsically disordered proteins are known to fulfill a great variety of crucial biological functions.[17–19] It has been suggested that the functional diversity provided by disordered regions might complement those of ordered protein regions.[11,17–19] Intrinsically disordered proteins were shown to have specific functions that can be grouped into four broad classes: (1) molecular recognition; (2) molecular assembly; (3) protein modification; and (4) entropic chain activities.[5]

A very important feature of the intrinsically disordered proteins or regions is their unique capability to fold under the variety of conditions. In fact, the folding of these proteins can be brought about by interaction with other proteins, nucleic acids, membranes or small molecules. It also can be driven by changes in the protein environment. The resulting conformations could be either relatively noncompact (i.e., remain substantially disordered) or be tightly folded.[7,9] There is evidence that many of these flexible proteins or regions undergo disorder-to-order transitions upon binding.[2–4,20]

While theoretical predictions suggest that a considerable fraction of proteome contains lengthy regions disordered in absence of binding partners,[4,13–15] experimentally confirmed cases of IDPs are still relatively scarce. Here we show that the metal-depleted form of pike parvalbumin, a protein being studied for more than 50 years, belongs to the family of IDPs, in accord with theoretical predictions.

Parvalbumin[21–24] is a small (Mr 12 kDa), acidic (pI 3.9–6.6), cytosolic Ca^{2+}-binding protein of the EF-hand superfamily (defined in PROSITE,[25] PDOC00018 entry), found in lower and higher vertebrates, including humans (for reviews see Refs. 26–29). It was detected in fast-twitch muscle cells, specific neurons of the central and peripheral nervous system, certain cells of several endocrine glands, and sensory cells of the mammalian auditory organ, the organ of Corti, and some other cells. The highest concentration of parvalbumin (up to several millimoles per liter) was found in fast muscles (mainly in skeletal, but sometimes in cardiac).[30,31] Parvalbumin was shown to serve as a soluble relaxing factor accelerating the Ca^{2+}-mediated relaxation phase in fast muscles, which was supported by direct gene transfer experiments[32] and by studies of parvalbumin knockout mice.[33] Parvalbumin, as well as calbindin, and calretinin, proved to be useful neuronal markers for a variety of functional brain systems and their circuitries (reviewed by Heizmann[34]). The exact functions of these proteins are still unknown, nevertheless their major role is assumed to be buffering, transport of Ca^{2+}, and regulation of various enzyme systems.

Parvalbumin, possessing two active EF-hand type Ca^{2+} binding sites, is frequently used as a model Ca^{2+} binding protein (reviewed in Ref. 35). It is convenient for studies of effects of interactions between two EF-hand binding sites and is very useful for studies of metal binding effects on interactions of protein with other proteins, peptides, membranes, and low molecular weight organic compounds, which frequently is of physiological significance. Moreover, parvalbumin forms several partially folded intermediate states, which have been widely studied by researchers interested in protein folding and stability problems, structural properties of intermediate molten globule-like states.

Amino acid compositions of parvalbumins are characterized by the following features (reviewed by Permyakov[29]), pointing out the possibility of intrinsic disorder: high content of Ala (9–29 per molecule), Lys (10–17 per molecule), Asp (8–15 per molecule), Glu (7–13), Leu (7–12), and Phe (8–10) residues; low content of Trp (0–1), Tyr (0–2), His (0–3), Pro (0–3), Met (0–3), Cys (0–3), and Arg (1–3 per molecule); acetylated N-terminus. Parvalbumin family evolutionarily diverged into two distinct sublineages, α and β (include oncomodulin),[36–38] differing in isoelectric points (α: pI $>$ 5; β: pI $<$ 5) and C-terminal helix length (1 residue longer in α). There are also at least 11 residues characteristically different between α and β forms of parvalbumin. A cysteine at position 18 and an aspartic acid at position 61 are characteristic of β-parvalbumins.[39]

The tertiary structure of both parvalbumin lineages is conserved over a wide phylogenetic range. The first structure of parvalbumin molecule (carp pI 4.25) was determined by Kretsinger *et al.* in 1973.[40–42] Parvalbumin is characterized by high content of α-helices (six segments, labeled A to F) and limited β-sheet structure. It consists of three homologous 30-residue-long segments each containing central loop flanked by short amphipatic α-helices, with hydrophobic side chains contributing to the core of the protein structure. The loops between the C and D helices and between E and F helices with flanking helices form two EF-hand type Ca^{2+}/Mg^{2+}-binding motifs (CD and EF sites). The loop between the A and B helices suffered a two-residue deletion that abolished metal binding affinity of the AB site. A characteristic feature of PA structure is a stabilizing salt bridge between conserved Arg75 and Glu81 residues, isolated from solvent by the N-terminal segment.

Two isoforms of parvalbumin are contained in skeletal muscles of northern pike (Esox lucius): parvalbumins pI 5.0 (pike III, α-isoform or α-PA: 0 Trp, 0 Tyr, 9 Phe, 0 Cys[43]) and pI 4.2 (4.1) (pike II, β-isoform or β-PA: 0 Trp, 1 Tyr, 10 Phe, 1 Cys[44]). Although the two proteins exhibit about 55% sequence identity and nearly identical peptide backbone conformations,[45–48] pike α-PA possesses two high affinity Ca^{2+} binding sites with similar calcium affinity, while pike β-PA has one similar high affinity Ca^{2+} binding site and one binding site with lowed affinity to Ca^{2+}.[49,50]

Information about Ca^{2+}-induced thermal stability changes of pike PAs is highly limited. Ca^{2+}-saturated (1 m*M* $CaCl_2$) form of β-PA was reported to exhibit two overlapping high temperature transitions, with mid-tran-

sition temperatures about 65–70°C and 87°C, respectively.[51] At the same time, apo-form of β-PA demonstrates a single thermal transition with half-transition temperature of about 20–24°C. All transitions are accompanied by the enthalpy change, which is characteristic for first-order phase transitions. The reported behavior is qualitatively identical to that observed for other representatives of parvalbumin family (reviewed in Ref. 35).

In this work we present a first study of physico-chemical properties of genuine metal-free parvalbumin. We demonstrate that metal-depleted forms of both pike PA isoforms lack first-order thermal transitions due to the absence of fixed tertiary structure. Nevertheless, apo-PA exhibit complex denaturation behavior, including presence of low temperature continuous phase transition, easily observed by means of near-UV CD. Opposite to β-isoform, apo-state of α-PA resembles the classical molten globule state. The absence of rigid tertiary structure is in line with both estimations of energetics of charge–charge interactions and sequence-based predictions of disordered chain regions of PA. Calcium saturation requirements for folding of apo-protein are established.

MATERIALS AND METHODS

Materials

Northern pike (*Esox lucius*) muscle parvalbumin isoforms α-PA and β-PA were isolated from pike white muscles as described.[52,53] The purity of protein samples was confirmed by native and SDS-PAGE, and checked spectrophotometrically, fluorimetrically, and using circular dichroism. Parvalbumin concentration was determined spectrophotometrically based upon molar extinction coefficients of $\varepsilon_{259\ nm} = 2699\ M^{-1}\ cm^{-1}$ for PA β-PA and $\varepsilon_{259\ nm} = 1810\ M^{-1}\ cm^{-1}$ for α-PA.[52,54]

HEPES, H_3BO_3 and glycine were ultra-grade, from Sigma Chemical (St. Louis, MO), Merck Biosciences, and Fluka, respectively. Guanidinium chloride was biochemistry grade from Merck Biosciences, EDTA standard solution from Fisher Scientific, $CaCl_2$ from Fluka. EDTA, EGTA, DTPA, and bis-ANS were bought from Sigma Chemical. Molecular mass markers for SDS-PAGE were purchased from Helicon (Moscow, Russia). Silver staining of SDS-PAGE gels was carried out using Amersham Biosciences PlusOne™ protein silver staining kit. Other chemicals were reagent grade or higher. All buffers and other solutions were prepared using nano-pure water (Millipore Simplicity 185 system).

Methods

Calcium removal from parvalbumin samples

Calcium removal from parvalbumin samples was performed using the Sephadex G-25 gel-filtration method described by Blum *et al.*,[55] where in some cases an excess of Ca^{2+} chelator (3 m*M* DTPA/EDTA) was used.

Scanning calorimetry measurements

Scanning calorimetry measurements were carried out on a DASM-4M differential scanning microcalorimeter (IBI RAS, Pushchino, Russia) at a 1°C/min heating rate in 10–20 m*M* H_3BO_3 or glycine buffer, pH 9.0. A pressure of three bars was maintained to prevent degassing of the solutions during heating. Protein concentrations were 1.6–2.1 mg/mL. The heat sorption curves were baseline corrected. Protein-specific heat capacity (C_p) was calculated as described by Privalov and Potekhin.[56] The partial molar volume and specific heat capacity of fully unfolded protein were estimated according to Hakel *et al.*[57,58] The temperature dependence of C_p was analyzed according to the simple two-state model, assuming that the difference between heat capacities of the denatured and native protein states (ΔC_p) is independent of temperature (all values were normalized by protein molecular weight MW):

$$C_p = C_{p,D} - \Delta C_p/(1+K) + \left[\frac{\Delta H_{VH} + \Delta C_p \cdot (T - T_0)}{T(1+K)}\right]^2 \cdot K/R, \quad (1)$$

where

$$K = \exp\left[\frac{\Delta H_{VH} - \Delta C_p \cdot T_0}{R}\left(\frac{1}{T_0} - \frac{1}{T}\right) + \frac{\Delta C_p}{R}\ln\frac{T}{T_0}\right] \quad (2)$$

$$R = 8.31/\mathrm{MW}\ \mathrm{J/(g\ K)}.$$

Here, T is absolute temperature and $C_{p,D}$ is the specific heat capacity of the denatured protein, linearly extrapolated to the transition region. Fitting parameters: ΔH_{VH} (van't Hoff's enthalpy of protein denaturation), T_0 (mid-transition temperature), and ΔC_p.

Circular dichroism (CD) measurements

Circular dichroism (CD) measurements were carried out with a JASCO J-810 spectropolarimeter (JASCO, Japan), equipped with a Peltier-controlled cell holder. The instrument was calibrated with an aqueous solution of d-10-camphorsulfonic acid (JASCO) according to the manufacturer's instruction. The cell compartment was purged with dry nitrogen (dew-point of −40°C) to avoid condensation of water vapors at lowered temperatures. Cuvettes with pathlengths of 10 and 1.00 mm were used for near- and far-UV regions, respectively. Protein concentrations were 130–220 and 5–11 μ*M* for near- and far-UV regions, respectively. The small contribution of buffer was subtracted from experimental spectra. Band width was 2 nm, averaging time 1–2 s, and accumulation 3. Quantitative

estimations of the secondary structure contents were made using the CDPro software package,[59] available at http://lamar.colostate.edu/~sreeram/CDPro. The experimental data in 190–240 nm range were treated by CDSSTR and CONTIN algorithms, using SDP48 and SMP56 reference protein sets. The final secondary structure fractions reported here represent the averaged values.

Temperature scans were performed at several wavelengths simultaneously in a stepwise manner, allowing the sample to equilibrate at each temperature. The average heating rate was 0.5°C/min. Band width was 2 nm, averaging time 8 s.

GdmCl-induced unfolding of parvalbumin was carried out using a set of solutions, containing equal amounts of the protein, differing by GdmCl concentration. Volumetric effects accompanying dilution of concentrated GdmCl stock solution were taken into account according to Kawahara and Tanford.[60] A minor contribution of GdmCl was subtracted.

Fluorescence studies were performed on a Cary Eclipse spectrofluorimeter (Varian), equipped with a Peltier-controlled cell holder and a precision automatic microtitrator (IBI RAS, Pushchino, Russia). Parvalbumin intrinsic fluorescence was excited at 259 nm; bis-ANS fluorescence was excited at 385 nm. Spectrofluorimetric temperature scans were performed stepwise allowing the sample to equilibrate at each temperature. Temperature was monitored directly inside the cuvette using Cary temperature probe (Varian). The average heating rate was 0.5°C/min. At temperatures below room temperature cell compartment was purged with dry nitrogen (dew-point of −40°C) to avoid condensation of water vapors.

Estimation of equilibrium Ca^{2+} association constants

The binding of Ca^{2+} ions to both pike parvalbumins can be successfully described by the sequential Ca^{2+} binding scheme[49]:

$$\begin{aligned} &\text{Protein} + Ca^{2+} \overset{K_1}{\Leftrightarrow} \text{Protein} \cdot Ca^{2+} \\ &\text{Protein} \cdot Ca^{2+} + Ca^{2+} \overset{K_2}{\Leftrightarrow} Ca^{2+} \cdot \text{Protein} \cdot Ca^{2+}, \end{aligned} \quad [1]$$

where K_1 and K_2 are Ca^{2+} binding constants for the two active EF-hands of parvalbumin.

The calcium affinity of parvalbumin was measured from spectrofluorimetric titration of the Ca^{2+}-free protein with a $CaCl_2$ standard followed by spectrofluorimetric titration of the Ca^{2+}-loaded protein with EDTA potassium salt at a fixed pH. Calculations of the Ca^{2+} association constants from the experimental data were performed considering the competition between the protein (scheme [1]) and the chelator for Ca^{2+} ions:

$$\text{EDTA} + Ca^{2+} \overset{K_{EGTA}}{\Leftrightarrow} \text{EDTA} \cdot Ca^{2+} \quad [2]$$

The Ca^{2+} association constant for EDTA, K_{EDTA}, was calculated according to Schwarzenbach and Flaschka.[61] The data were globally fitted using FluoTitr v.1.2 software written in Delphi 2005 programming language (Borland® Software Corporation), implementing nonlinear regression algorithm by Marquardt.[62] The fit was achieved by variation of the binding constants K_1 and K_2. The quality of the fit was judged by the randomness of residuals distribution. The resulting accuracy of the Ca^{2+} binding constants was about $\pm 1/4$ orders of their magnitudes.

Electrostatics calculations

The energies of charge–charge interactions were calculated using the finite difference Poisson-Boltzmann (FDPB) method as implemented in the DelPhi module[63] of the Insight II molecular modeling environment (Insight II 2005, Accelrys Software, San Diego). Calculations were performed for X-ray structures of pike α-PA (PDB code 1PVA, chain A[47,48]) and β-PA (PDB code 1PVB[45–47]). Water molecules were excluded from both structures, one ammonium ion from β-PA. Ionic strength of the solvent (dielectric constant 80.0, molecule radius 1.4 Å) was set to zero. The solute extent was 80%, number of grid points—33. Debye-Hückel-type boundary conditions were used. DelPhi's default charge and radius templates were used. The charges of atoms subjected to estimation of electrostatic potential were selectively set to zero.

Predictions of intrinsic disorder

Predictions of the intrinsic disorder propensity were performed using the recently developed various short-long, version 1 predictor of natural disordered regions (PONDR®-VSL1), which is an ensemble of logistic regression models that predict per-residue order-disorder.[64,65] Two models predict either long or short disordered regions—greater or less than 30 residues. The algorithm calculates a weighted average of these predictions, where the weights are determined by a meta-predictor that approximates the likelihood of a long disordered region within its 61-residue window. Predictor inputs include PSI-blast profiles,[66] and PHD,[67] and PSI-pred[68] secondary structure predictions.

RESULTS AND DISCUSSION

Metal removal from pike parvalbumin

Parvalbumin is a protein with one of the highest affinities for Ca^{2+} ions, with equilibrium Ca^{2+} association constant (K_{Ca}) reaching 1×10^{10} M^{-1} for some members of PA family (for review see Ref. 35). For pike parvalbumin, K_{Ca} was shown to reach 6×10^8 M^{-1} at pH 8 and 20°C.[49] Figure 1 depicts the temperature depend-

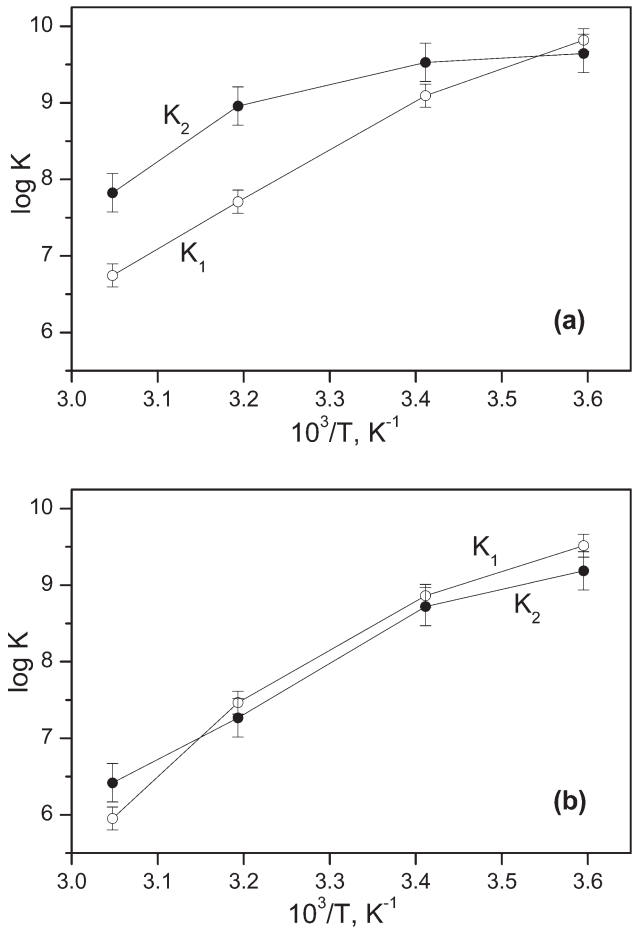

Figure 1

*Temperature dependence of equilibrium Ca^{2+} association constants for pike parvalbumin isoforms α-PA (pI 5.0) (**a**) and β-PA (pI 4.2) (**b**), estimated from spectrofluorimetric Ca^{2+}/EDTA titrations of apo-protein as described in,[49] according to the sequential Ca^{2+} binding scheme [1]. Buffer conditions: 10–20 mM HEPES-KOH, pH 8.0–8.2. Concentration of PA was 8–14 μM.*

ence of K_{Ca} values for pike parvalbumin isoforms α-PA (a) and β-PA (b), estimated from spectrofluorimetric Ca^{2+}/EDTA titrations of apo-protein as described in Ref. 49, according to the sequential Ca^{2+} binding scheme [1]. The highest K_{Ca} value, achieved at 5°C, equals to 7×10^9 M^{-1}. It implies that special precautions should be taken to ensure complete removal of Ca^{2+} ions from PA in the whole temperature range to be studied. The method described by Blum *et al.*,[55] using Sephadex G-25 gel-filtration, is an efficient tool for nearly complete Ca^{2+} depletion from PA. Meanwhile, the use of background millimolar level of strong Ca^{2+} chelators (EDTA, DTPA, etc.) is an additional highly efficient way to secure apo-protein from contaminating calcium. This approach requires an appropriate relation between pH value of the solution and chelator to protein molar ratio.

The pH range 8.0–9.0 was used in the present work since no other observable pH-transitions in pike parvalbumins were monitored in this range by intrinsic fluorescence for both PA isoforms and tyrosinate absorbance for PA 4.2,[49] and chemical shifts of C2H and C5H protons of histidine residues of PA 5.0 (His 25 and 106).[69] If the Ca^{2+} removal procedure described by Blum *et al.*[55] was skipped then millimolar concentrations of EDTA or DTPA were used at pH near 9 (lowering of pH would decrease apparent K_{Ca} values), were both chelators possess K_{Ca} values around 1×10^9 M^{-1}.[61] Apparently, about two orders of magnitude molar excess of chelator over metal binding sites of PA is required to ensure efficient removal of two Ca^{2+} ions from the protein, exhibiting K_{Ca} values about 7×10^9 M^{-1} (see Fig. 1). Intrinsic fluorescence experiments did not reveal EDTA or DTPA (potassium salts) binding to pike PA up to 3 m*M* chelator concentration (data not shown), so the chelators concentrations were kept within this limit.

An important property rarely taken into account upon experimental studies of parvalbumins is their relatively high affinity to Na^+ ions. For pike PAs an effective sodium binding constant was shown to be 36–39 M^{-1} at pH 8 and 20°C.[49,70] According to our present estimations it equals 37 M^{-1} for α isoform, and 14 M^{-1} for β-form. It means that application of Na^+ as a counter ion in the buffer systems used for studies of apo-protein would be accompanied with partial loading of metal binding site(s) of PA with sodium ions. Considering that an apparent K^+ association constant for pike PAs is 9–19 M^{-1} at pH 8 and 20°C[49,70] and even less (4–5 M^{-1}), according to our present observations, potassium is more suitable for achievement of high quality apo-PA. Thus, sodium was excluded from the buffer systems used in this study, instead minimal levels of potassium ion were used.

The absence of first-order thermal transitions for apo-form of pike parvalbumin

Strictly speaking, the thermal transition in a protein can not be considered as a classical phase transition, since certain distinctive features of phase transitions considered in classical physics, like the presence of phase boundary, are absent in this case. Here, the term "phase transition" is applied to intramolecular transitions occurring within a protein molecule in response to temperature change.

According to the modern classification of phase transitions the first-order phase transitions are those that involve a latent heat. During such a transition, a system either absorbs or releases a fixed amount of energy, which can be directly observed by means of thermophysical methods of investigation. The scanning microcalorimetry data obtained for metal-depleted forms of pike PAs [Fig. 2(a,b)] did not reveal any measurable excess heat

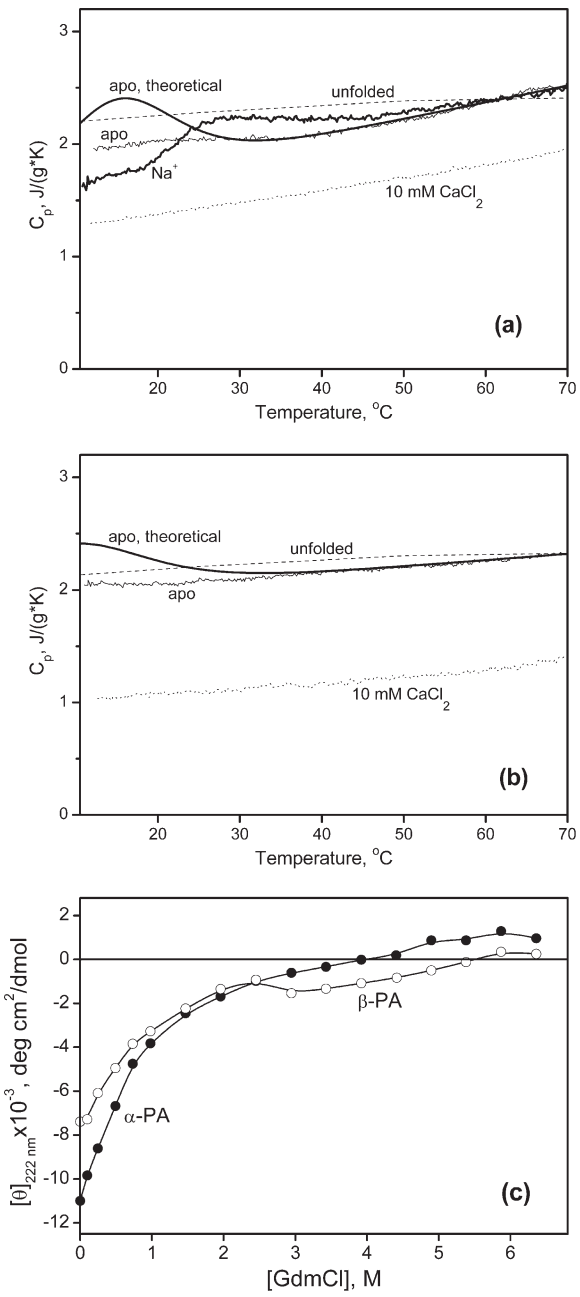

Figure 2

*The thermally and guanidinium chloride-induced unfolding of apo-forms of pike parvalbumins, monitored by DSC and CD. Temperature dependence of specific heat capacity of pike parvalbumin isoforms α-PA (**a**) and β-PA (**b**), estimated from DSC data (10 mM H_3BO_3 or 20 mM glycine, pH 9.0; heating rate 1 K/min). Concentration of PA was 1.6–2.1 mg/mL. Apo-form of PA was prepared using the Sephadex G-25 gel-filtration method described by Blum et al.[55] Apo-α-PA was measured in the presence of 3 mM DTPA chelator. K^+ was used as a counter ion in the buffer system. Na^+-loaded form of α-PA was achieved by using Na^+ as a counter ion in the buffer system in the presence of 3 mM EDTA. Dashed curve corresponds to the heat capacity of fully unfolded PA, as estimated according to Hackel et al.[57] The theoretical melting curve for the apo-PA was reconstructed from the near-UV CD data [see Fig. 3(c)], based upon a two-state model [see Eqs. (1) and (2)]. GdmCl-induced unfolding of apo-forms of pike parvalbumins (**c**) α-PA (solid circles) and β-PA (open circles) at 20°C, traced by molar ellipticity at 222 nm (10 mM H_3BO_3, pH 8.9, 1.5 mM EDTA). K^+ was used as a counter ion in the buffer system. Protein concentrations were 5–6 μM.*

sorption peaks characteristic for the first-order thermal transitions. Furthermore, the specific heat capacity of apo-protein, $C_{p,apo}$, significantly exceed the values observed for Ca^{2+}-saturated PA (10 m*M* $CaCl_2$), which is folded in this temperature range.[51] The $C_{p,apo}$ values are closer to the heat capacity of fully unfolded PA, as estimated according to Hackel *et al.*[57] [Fig. 2(a,b)]. Thus, the protein-specific heat capacity absolute values, which can be regarded as a measure of hydration of its amino acid residues,[71] argue that apo-PA is essentially solvated and, consequently, lacks rigid tertiary structure. Thus, the DSC data evidence the absence of first-order thermal transitions in the apo-form of pike PA due to the lack of fixed tertiary structure. The latter is supported by guanidinium chloride-induced unfolding experiments at 20°C [Fig. 2(c)]. The absence of any plateau at the very beginning of the denaturation curve implies that the protein structure is unable to withstand the denaturant action, the behavior characteristic for nonrigid, fluctuating structure. Both DSC and GdmCl studies unambiguously evidence that apo-parvalbumin does not possess rigid tertiary structure and therefore is an intrinsically disordered protein.

Importantly, the use of Na^+ instead of K^+ as a counter ion in the buffer system causes partial loading of the metal-binding site(s) of PA with sodium (discussed above), resulting in the protein folding (as confirmed by the decrease in specific heat capacity) and appearance of the marked excess heat sorption peak with an apparent half-transition temperature of about 27°C [Fig. 2(a)]. This result is similar to the observation reported earlier for "apo-form" of pike β-PA in the presence of 100 m*M* KCl[51]: in this case a single excess heat sorption peak was also detected, with mid-transition temperature of about 22°C. Taking into consideration that under these conditions the apparent K^+ association constant for pike PAs is 13–19 M^{-1} [49,70] (4–5 M^{-1}, as estimated in the present study), the 100 m*M* level of KCl was enough for partial loading of the protein with potassium ions. Thus, the enthalpy effects accompany the thermal denaturation of Na^+- or K^+-bound forms of pike parvalbumin, while the genuine apo-form of parvalbumin exhibits the absence of any first-order transitions [Fig. 2(a,b)].

It should be noted that the general practice in studies of physico-chemical properties of parvalbumins and other calcium binding proteins is the addition from tens up to 250 m*M* of NaCl or KCl (reviewed in Ref. 35) to model physiological ionic strength levels. For this reason most of the data reported so far for "apo-parvalbumins" actually relate to sodium- or potassium-bound forms of the protein. For example, in the works of Henzl and coworkers,[72–75] Ca^{2+}-free forms of oncomodulin, α and β isoforms of rat parvalbumin, avian β-parvalbumin, and parvalbumin isoform 3 (PV3) from chicken were studied in the presence of 200 m*M* NaCl, preventing from achievement of genuine apo-protein. Similarly, in

the work of Williams *et al.*,[76] Ca^{2+}-depleted form of rat α-parvalbumin contained 200 m*M* KCl. In some studies the addition of NaCl or KCl was avoided but excess of disodium salt of EGTA/EDTA was used for removal of Ca^{2+} ions. For example, in the study by Filimonov *et al.*[77] apo-form of carp parvalbumin pI 4.25 was investigated in the presence of 5 m*M* Na_2EDTA. In some studies the type of chelator salt used is not specified, making impossible to evaluate Na^+ and K^+ content. For all the situations, unfavorable with respect to achievement of real metal removal from PA, the available DSC data evidence a single excess heat sorption peak. Similarly to pike parvalbumins, the complete removal of Na^+ cations from the buffer systems used and minimal levels of K^+ ion probably would result in disappearance of the heat effects, accompanying thermal denaturation of other "Ca^{2+}-depleted" parvalbumins. To the best of our knowledge, cases of this kind were not reported so far. Therefore we assume that present work is a first rigorous study of genuine metal-free parvalbumin.

Complex denaturation behavior of apo-parvalbumin

Although differential scanning calorimetry measurements revealed the absence of distinct heat sorption peak for apo-form of pike PA, spectroscopic techniques evidence its quite complicated temperature-dependent behavior, reflecting the presence of certain temperature induced changes in the protein structure (see Fig. 3). While far-UV region circular dichroism measurements did not reveal the presence of any cooperative thermal transitions in metal-depleted pike β-PA [Fig. 3(b)] (the same situation is observed on other wavelengths studied), α-isoform exhibits the U-shaped thermal changes of molar ellipticity [Fig. 3(a)], with extremum in the range of 20–30°C (depending upon the wavelength). The same experiment performed for the Ca^{2+}-loaded α-PA (not shown) has confirmed the absence of any changes in this temperature range. This behavior of apo-PA resemble the effects observed in the case of cold denaturation, which could imply that some minor fraction of α-PA remains folded at 20–30°C, where maximum protein stability is achieved. Alternatively, this phenomenon could be attributed to the cold denaturation of the disordered protein state.

The temperature dependencies of extrinsic fluorescence of hydrophobic probe bis-ANS (protein to probe molar ratios 5–10) [Fig. 3(a,b)] does not reveal evident effects down to 6°C except trivial thermal quenching. Taking into consideration that bis-ANS fluorescence intensity for apo-α-PA is about 60 times (20°C) higher than that for the folded protein (Ca^{2+}-loaded form), formation of a folded form of apo-state during thermal denaturation at 20–30°C would be accompanied with substantial decrease in bis-ANS fluorescence. The absence of such changes in this temperature range indicates that the U-shaped changes of molar ellipticity with temperature are most likely due to the cold denaturation of the apo-α-PA state lacking rigid tertiary structure.

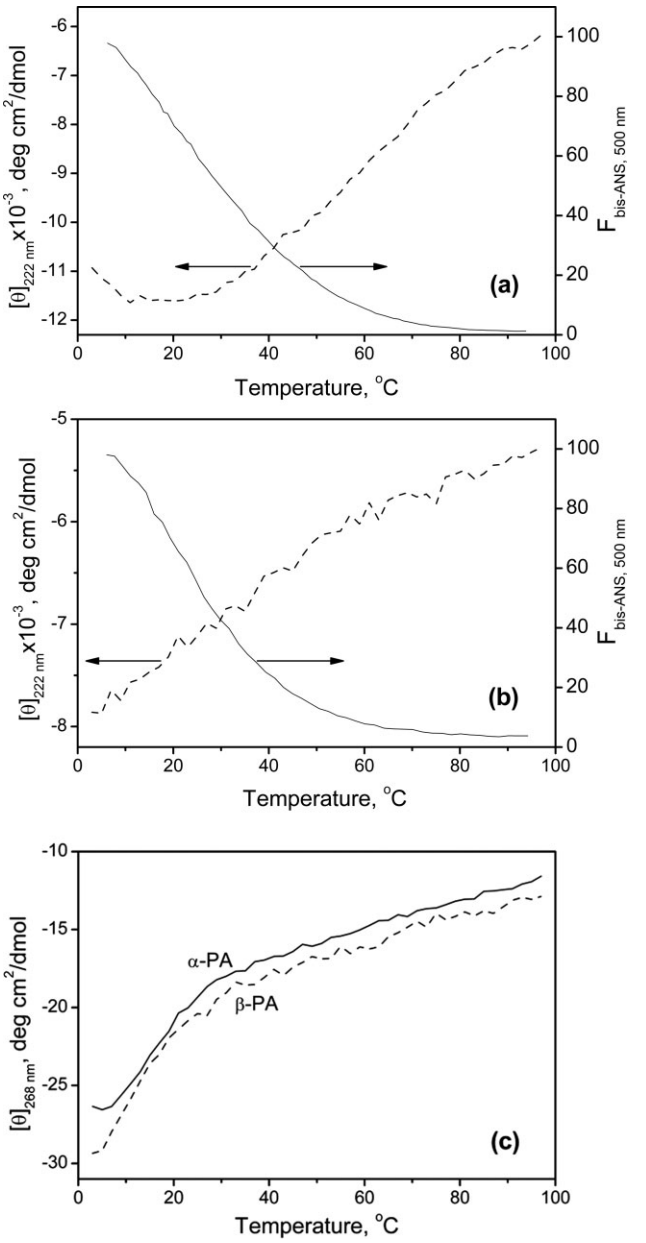

Figure 3

*Thermal denaturation of apo-forms of pike α-PA (**a**) and β-PA (**b**), monitored by far-UV CD (dashed curves) and bis-ANS fluorescence (solid curves, arbitrary units), and near-UV CD (**c**). Buffer conditions: 10 mM H_3BO_3, pH 8.7, 1.5–2.7 mM EDTA or 10–20 mM HEPES, pH 8.2, 3 mM EDTA, for near-UV CD. In the near-UV experiments Ca^{2+} was depleted using the gel-filtration method described by Blum et al.[55] K^+ was used as a counter ion in the buffer systems. Protein concentrations were 5 μM for far-UV CD, 9–20 μM for fluorescence measurements, and 0.13–0.2 mM for near-UV CD. Bis-ANS concentration was 2 μM. The excitation wavelength was 385 nm.*

The unusual thermal denaturation behavior of the metal-depleted pike PA is evident from the examination of the temperature dependencies of near-UV molar ellipticity [Fig. 3(c)], demonstrating cooperative changes from 3 to 30°C (absent for the Ca^{2+}-loaded forms) with midpoint about 10–15°C, resembling those observed for typical first-order phase transitions, however, the absence of detectable heat sorption peaks in the course of this thermal transition [Fig. 2(a,b)] shows that the observed spectral changes correspond to phase transitions, different from the first-order transitions. To emphasize the difference between the experimental DSC data for apo-PA [Fig. 2(a,b)] and those expected for a first-order transition, possessing the cooperativity of the thermal transition observed in circular dichroism transition curves [Fig. 3(c)], a theoretical DSC melting curve for the apo-PA was reconstructed from the near-UV CD data, based upon a two-state model [see Eqs. (1) and (2)] [Fig. 2(a,b)]. The comparison of these two curves confirms that the experimental accuracy of specific heat capacity determination was sufficient to discriminate between the two types of phase transitions.

The found here absence of latent heat during phase transition is an indication of continuous or second-order phase transition.[78] The transitions of this kind are qualitatively different from the first-order transitions. In such transitions different phases do not coexist at the transition point. Instead, system state changes continuously during the second-order transition. As a result, there is no discontinuity in the thermodynamic functions of the system at the transition temperature. Meanwhile, discontinuity of heat capacity, and other derivatives of thermodynamic functions of the system is characteristic for the second-order transition. Some of the non-first order transitions observed in proteins indeed exhibit heat capacity change during transition. For example, thermal denaturation of acidic form (pH 4.4) of apomyoglobin is accompanied by marked heat capacity change, as observed in DSC experiment.[79] At the same time, in our case and for acidic form of α-lactalbumin[80] the discontinuity of heat capacity seems to absent, which may imply that they are different in the underlying nature. Thus, protein phase transitions lacking latent heat can be different from the continuous (or second-order) phase transition considered in classical physics. Proteins are drastically different from the classical physical systems, which gave rise the definition of the second-order phase transitions, in that they are small (so only intramolecular phase transitions can take place), much more heterogeneous by composition and do not possess the required level of symmetry. All these factors greatly complicate the direct extension on proteins of the principles formulated for continuous phase transitions in classical physics. A creation of a separate formalism, enabling rigorous consideration of continuous transitions in proteins is therefore required. Nevertheless, taking into account that their peculiarities are still far from being well studied, we will refer to transitions of this kind as continuous just on the basis of the absence of latent heat.

Importantly, the near-UV CD changes for apo-α-PA [Fig. 3(c)] show the signs of cold denaturation, in concert with the far-UV molar ellipticity changes [Fig. 3(a)]. To reveal details of the thermal transitions monitored for apo-PA by circular dichroism spectroscopy, a highly informative approach was applied: construction of a phase plot (see Fig. 4), representing a dependence of the far-UV CD signal upon the near-UV CD signal, obtained at the same temperature. The method was first introduced by Burstein[81,82] for protein fluorescence data analysis, but can be easily extended on any other parameter, linearly related with populations of system's states.[83,84] Each straight line in the phase plot corresponds to a transition between two protein conformations. Thus, experimental conditions at which separate protein states are achieved

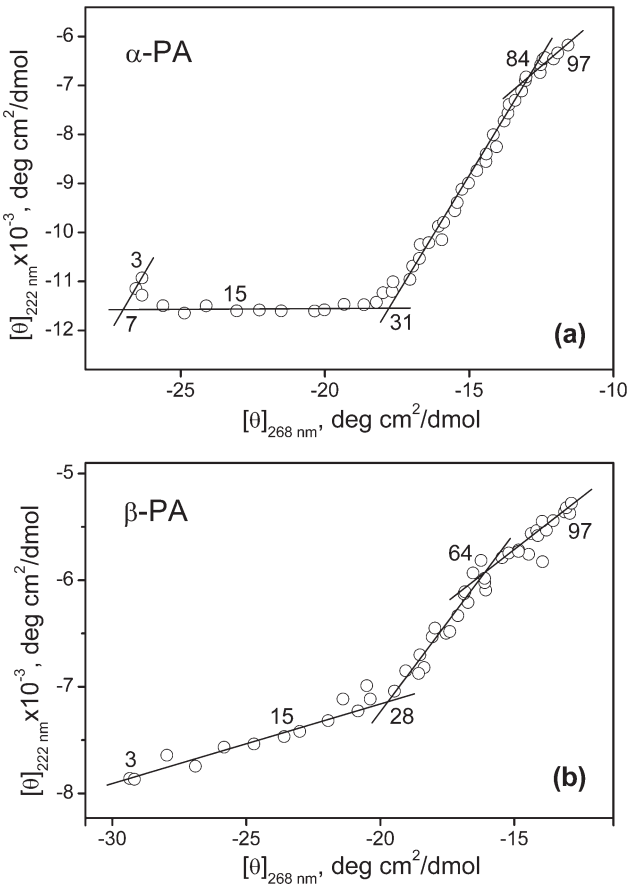

Figure 4

*Phase plot analysis of the temperature-induced denaturation of metal-depleted pike isoforms α-PA (**a**) and β-PA (**b**), based on the near and far-UV CD data, shown in Figure 3. Each straight line represents a transition between two conformations of the protein. The temperature values corresponding to the key points of the phase plots are indicated.*

and the areas of transitions between them are localized with ease. Application of this approach to the CD data shown on Figure 3 demonstrates that at least 3 (α-PA) or 2 (β-PA) intermediates are observed in the course of the thermal transitions of pike apo-PA (see Fig. 4). One of them is observed at temperature about 30°C and is characterized by high content of α-helical structure and markedly increased symmetry and mobility of the environment of aromatic groups. Another one, detected at 84°C (α-PA) or 64°C (β-PA), demonstrate notably decreased helical content and further increased mobility of aromatic groups environment. One more intermediate is observed at temperature about 7°C for α-PA. It is characterized by high content of α-helical structure along with more rigid environment of its aromatic residues, thereby representing the most structured intermediate.

The phase plots on Figure 4 reveal that the continuous transition observed by near-UV CD [Fig. 3(c)] is not accompanied with gross changes in α-helical structure. Minor changes are observed in the case of β isoform. It means that the continuous transition affects the environment of aromatic groups of PA, while its secondary structure remains substantially unchanged. This may imply that the transition is caused by rearrangements in very limited regions of the secondary structure or by disruption of the remaining residues contacts between the fairly stable elements of the secondary structure. For example, similar transition observed for acidic form of α-lactalbumin[80] was shown to be accompanied, if not caused, by cooperative structural rearrangement in 3_{10}-helix loop.

It should be noted that thermal denaturation of apo-PA results in relatively moderate secondary structure changes. Application of just 0.4–0.5 *M* of guanidinium chloride at 20°C [Fig. 2(c)] causes the same ellipticity changes as heating up to 97°C [Fig. 3(a,b)]. Further denaturation with GdmCl is accompanied with manifestation of multiple structural transitions [Fig. 2(c)]. A quite unusual phenomenon, observed at maximal GdmCl concentrations is the positive molar ellipticity at 222 nm, which on one hand is expected for random coil-like structure, but on the other hand, is rarely observed experimentally. This means that GdmCl-induced denaturation of apo-PA results in nearly complete unfolding of the polypeptide chain. Overall, the circular dichroism data on thermal and denaturant-induced unfolding of apo-PA evidence the presence of numerous intermediates, which imply that different elements of its secondary structure possess different resistance with respect to the denaturing factors of the environment.

Structural characterization of apo-parvalbumin

As was shown above, metal-depleted forms of both pike PA isoforms reach the most structured state at low temperatures (see Fig. 4). It is of interest to compare structural properties of this state with the fully folded protein, which can be obtained upon Ca^{2+}-binding.[51] Far- and near-UV CD spectra for apo- and Ca^{2+}-loaded (1 m*M* $CaCl_2$) forms of α and β PAs at 3°C are compared on Figure 5. Estimations of secondary structure contents for the Ca^{2+}-saturated PAs using the CDPro software package[59] shows fairly good agreement between the CD-based values of α-helices content and those derived from the respective crystal structures: 54% (CD) versus 57% (PDB code 1PVA[47,48]) for α-PA, and 58% (CD) versus 56% (1PVB[45–47]) for β-PA. The removal of metal ions from the proteins is accompanied with the α-helical structure loss: by 8% for α-PA and by 30% for β isoform. Thus, much more prominent changes are observed for β-PA. The decrease of helices content in α isoform is accompanied by nearly equal increase in the content of β-pleated structure and turns. The same effect for β-PA is mostly (14%) due to the increase in unordered structure content, with the remaining changes being shared between β-sheets and turns. Although circular dichroism technique is not very reliable in the estimation of the contents of the secondary structure elements, different from α-helices, one may expect that the secondary structure of the metal-free form of α-PA is nearly identical to the Ca^{2+}-loaded protein, whereas β isoform is essentially (ca. 38%) disordered.

The Ca^{2+} association induces in α-PA a pronounced spectrally uniform increase of negative molar ellipticity in the near-UV region (see Fig. 5), which is indicative of less symmetric and mobile environment of its Phe residues. This behavior is in full accord with previously described observations, evidencing that apo-PA lacks specific tertiary structure. At the same time, β isoform demonstrates less obvious behavior. The CD spectrum in the Phe spectral range is less pronounced and its magnitude is comparable to that for apo-α-PA irrespective of Ca^{2+} content, which suggests that Phe residues of β-PA are located in a quite mobile environment even in the folded state. The Ca^{2+}-binding causes a shift of CD spectrum's extremums, with the difference spectrum exhibiting in the Phe region two positive bands with maxima at 259.6 and 266.3 nm and a single negative band at 263.4 nm. The last two extremums correspond to the absorbance bands of Phe residues. Thus, the CD data evidence that the environment of Phe residues in β-PA undergo relatively limited changes upon denaturation, which is quite unexpected. Meanwhile, the surroundings of its single Tyr47 residue expectedly become more mobile, as confirmed by ellipticity increase in the Tyr spectral range. Overall, the near-UV CD spectra imply that apo-forms of both PA isoforms retain some native-like residue contacts, which disrupt in multiple steps upon thermal denaturation [Figs. 3(c) and 4]. Heating up to 97°C causes about 2.3-fold decrease of molar ellipticity magnitude at 268 nm. Thus, as was observed for secondary structure

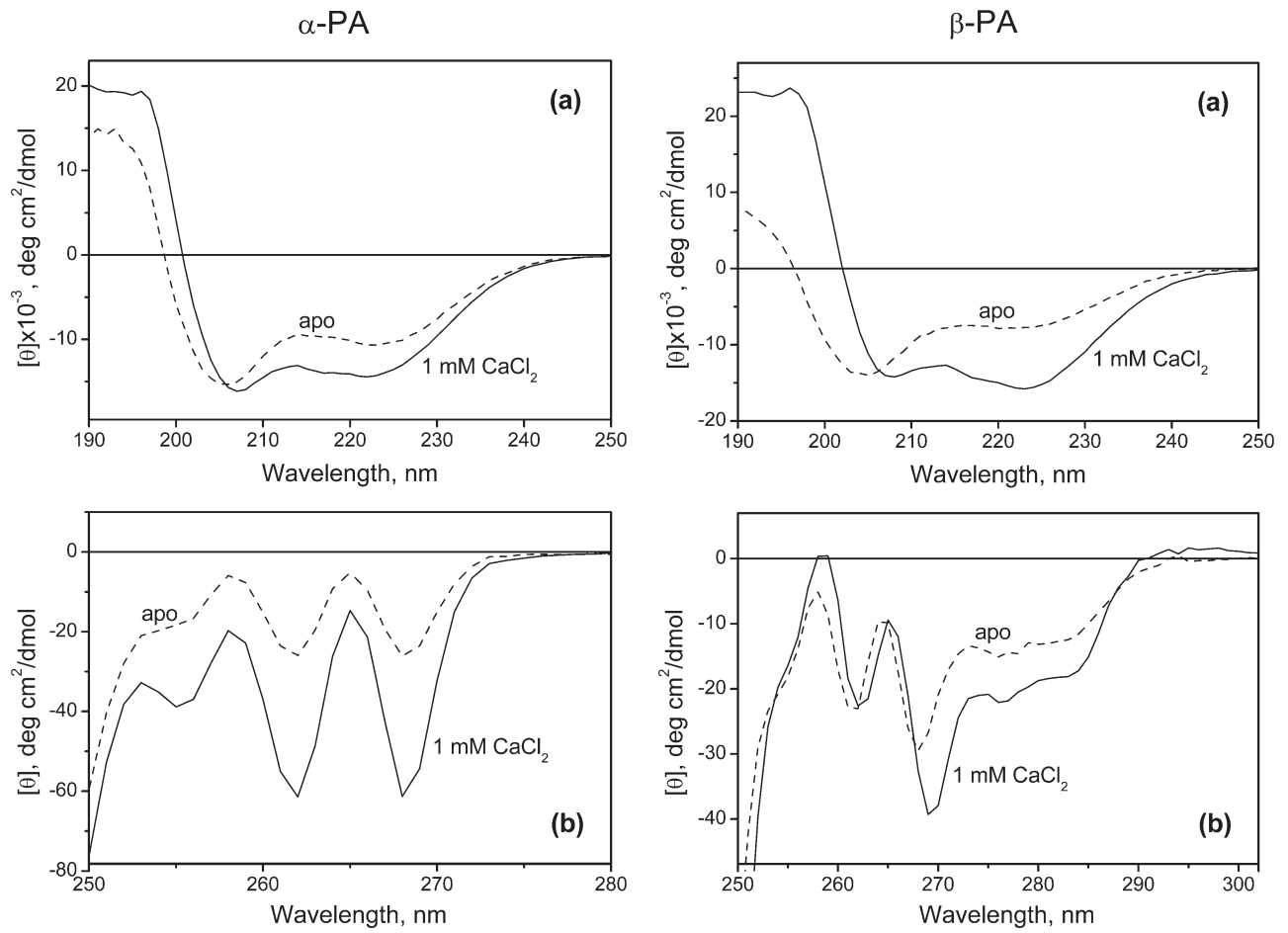

Figure 5

*Far- (**a**) and near-UV (**b**) CD spectra for apo- and Ca^{2+}-loaded (1 mM $CaCl_2$) pike α-PA and α-PA at 3°C. Protein concentrations were 5–11 μM and 130–220 μM for far- and near-UV regions, respectively. Buffer conditions: 10 mM H_3BO_3, pH 8.9 (far-UV region and near-UV experiment for Ca^{2+}-loaded β-PA) or 10–20 mM HEPES, pH 8.2. In the near-UV CD experiments Ca^{2+} was depleted using the gel-filtration method described by Blum et al.[55] in the presence of 3 mM EDTA, while in the far-UV experiments 1.5 mM EDTA was applied. K^+ was used as a counter ion in the buffer systems.*

changes upon heating, the heating up to 97°C does not cause complete elimination of the native-like residues contacts.

Comparison of the present CD spectra with those available in literature[50,85,86] shows that Ca^{2+}-induced CD changes measured in our work both in the far- and near-UV regions are much more pronounced. The difference seems to be due to the fact that metal ion content was controlled much more carefully in our experiments, ensuring achievement of high quality metal-free form of parvalbumin.

Taken together, the experimental data on apo-α-PA manifest the whole set of hallmarks of the classical molten globule state.[87–89] First of all, it does not possess a first-order thermal transition. Moreover, the removal of Ca^{2+} ions from the α-isoform is accompanied with relatively limited changes in its secondary structure and concomitant increase in the mobility of the environment of its Phe residues. Finally, bis-ANS fluorescence intensity for apo-α-PA is about 60 times (20°C) higher than that for the folded protein, the behavior characteristic for a molten globule state (see Ref. 12 for review). Somewhat different situation is observed for apo-β-PA. Although it does not exhibit a first-order thermal transition, and its bis-ANS fluorescence intensity is about six times (20°C) higher compared with that for the folded PA, its secondary structure is drastically disordered. The latter does not allow classifying this state as a classical molten globule. Meanwhile, the direct experimental data on hydrodynamic radii of both parvalbumin isoforms are required in order to discriminate between the molten globule state and less compact structural states.

The known cases of continuous phase transitions in proteins were reported for molten globule or similar states,

possessing high content of residual secondary structure. Second-order transitions were observed for the molten globule states of α-lactalbumin[80] and apomyoglobin.[79] Structural transition of second-order type was reported for the denatured state of Engrailed Homeodomain demonstrating molten globule-like properties.[90] Our results follow this trend. The presence of a pronounced secondary structure seems to be one of the requirements for manifestation of transitions of this kind. One could assume that the continuous transitions occur at the secondary structure level or due to disruption of the remaining links between stable elements of the secondary structure. Probably, continuous phase transitions may occur also in proteins possessing rigid tertiary structure and some elements of disordered structure, but their observation is seriously complicated in this case.

Estimations of energetics of charge–charge interactions in pike parvalbumins

Calculations of the energies of the charge-charge interactions in the parvalbumins were carried out using the FDPB method as implemented in the DelPhi module[63] of the Insight II molecular modeling environment for two forms of each pike parvalbumin isoform: Ca^{2+}-loaded protein (X-ray structures 1PVA (chain A) or 1PVB), and apo-form based on the 1PVA or 1PVB structures with Ca^{2+} ions excluded from the calculations. Comparison of the results of these calculations (see Fig. 6) reveals several features, valid for both PA isoforms:

1. The AB domain (residues 1–40) is electrostatically inactive, exhibiting low energies of charge–charge interactions. β-PA has relatively low density of charged residues in this region. On the contrary, the CD and EF domains demonstrate the presence of multiple charges, giving significant contributions into electrostatic interactions of the protein.
2. The energy contributions of the charges of the conserved Arg74(75) and Glu80(81) residues, involved into the salt bridge, are strongly stabilizing without regard to Ca^{2+} binding. The fact was shown experimentally[92] and the absence of sensitivity to calcium seems to be a consequence of fairly large distance (ca. 20 Å) between these residues and Ca^{2+} ions.
3. In the apo-state many acidic side chains possess highly unfavorable charge–charge interactions: D50, D52, E58, E61, D89, D91, D93, and E100. They are all located within the functional EF-hand loops 50–61 (CD-loop) and 89–100 (EF-loop), being directly involved into Ca^{2+} coordination. Thus, the electrostatic repulsion between the negative charges of carboxylic groups coordinating calcium ion should greatly destabilize apo-PA structure.
4. Evidently, Ca^{2+}-binding has the most pronounced effect on residues directly coordinating Ca^{2+} ions. For each of these residues the charge-charge interaction energy, being large and unfavorable in the apo-form, becomes comparably favorable upon Ca^{2+} association. As a result, electrostatic interactions in the Ca^{2+}-bound PA are almost exclusively favorable, which seems to rationalize the very high stability of the Ca^{2+}-loaded protein.[49]

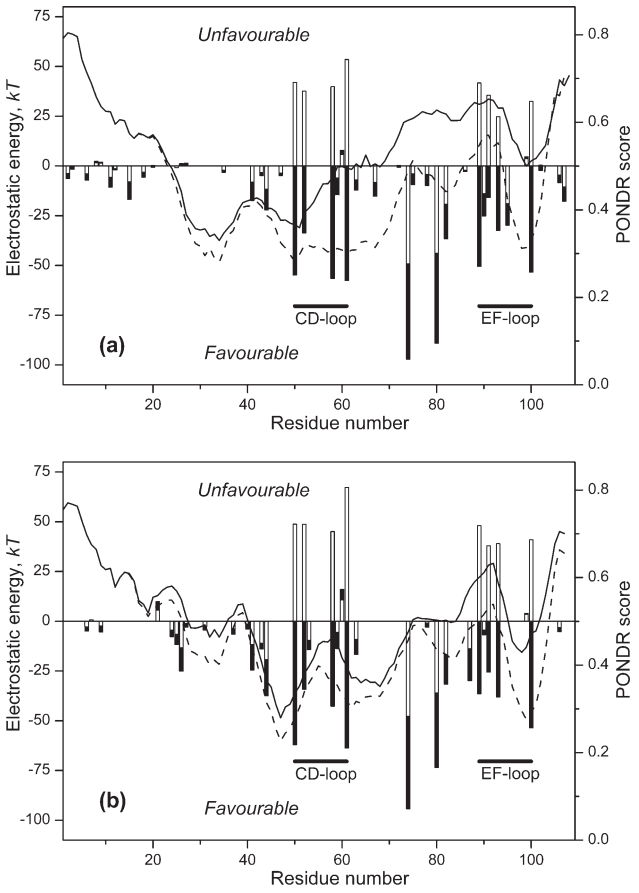

Figure 6

*Energies of the charge-charge interactions (bars) and PONDR scores (solid curves) for pike α-PA (**a**) and β-PA (**b**). The energies of charge-charge interactions were calculated using the FDPB method as implemented in the DelPhi module[63] of the Insight II molecular modeling environment; X-ray structures of α-PA (PDB code 1PVA, chain A) and β-PA (PDB code 1PVB[45]) were used. Calcium ions were either left in place (black bars) or removed (white bars). PONDR® VSL1 protein disorder predictor[91] was used. Dashed curves are calculated for parvalbumin forms in which the Ca^{2+}-coordinating Asp and Glu residues are substituted by Asn and Gln, respectively.*

Although the present analysis of electrostatic interactions within apo-parvalbumin molecule is based upon the Ca^{2+}-bound protein structure, it demonstrates a pronounced electrostatic destabilization of the folded state of apo-PA. Apparently, a conformational transition towards more thermodynamically favorable state should be anticipated. The experimental data presented here show that parvalbumin loses its rigid tertiary structure during this structural rear-

rangement. Evidently, this circumstance may be the reason why apo-PA three-dimensional structure is not solved so far.

Sequence-based predictions of disordered regions in pike parvalbumin

Figure 6(a,b) represent PONDR VSL1 curves for pike parvalbumin isoforms α and β, respectively. To evaluate the disorder propensities of parvalbumin forms lacking Ca^{2+}-coordinating negative electrostatic charges, the same calculations were performed for "discharged" PA forms, in which the Ca^{2+}-coordinating Asp and Glu residues within the EF-hand loops 50–61 (CD-loop) and 89–100 (EF-loop) were substituted by Asn and Gln residues, respectively. Figure 6 shows that both α-PA and β-PA possess high propensity for intrinsic disorder, as more than 50% of their residues are identified as disordered (their corresponding PONDR VSL1 scores are above the 0.5 threshold). In fact, PONDR VSL1 predicts that apo-forms of α-PA and β-PA might have 61 and 53% disordered residues, respectively. The situation changes dramatically for "discharged" forms, predicted to have significantly lower amount of disordered residues, ~34% for both PAs. Such excess negative charge compensation in the Ca^{2+}-loops of PAs affects mostly the central and C-terminal regions of both proteins, whereas their N-termini remain substantially disordered. These changes are more pronounced in the α-PA. This is reflected not only in the smaller number of residues with high disorder score in the "discharged" α-PA, but also in a more pronounced gap between the PONDR VSL1 curves calculated for the "discharged" and original forms of this protein. The charge compensation-induced changes in PONDR score support the hypothesis that the instability of apo-parvalbumin and its intrinsic disorder are determined by the unfavorable charge-charge interactions within Ca^{2+}-binding loops of the protein.

Similarly, the unfavorable electrostatic interactions within EF-loops are accompanied with high PONDR score values. A local maximum of the PONDR score corresponds to the CD-loop of β-PA. At the same time, the N-terminal part (1–20) of both PA isoforms is predicted to be strongly disordered, while being essentially electrostatically inactive. Besides, the region around the highly favorable electrostatically salt bridge between Arg74(75) and Glu80(81) residues demonstrates a high disorder propensity. Hence, only partial correlation between the disorder propensities and the charge-charge interaction energies is observed. The charge-charge interactions alone can not explain all extremums of the PONDR score and certain other factors may come into play here.

Ca^{2+}-induced refolding of apo-form of pike parvalbumin

Taking into consideration that Ca^{2+}-binding experiments on pike PA are well described by the sequential mechanism of filling of the protein binding sites[49] (see Fig. 1), it is of importance to know whether or not both sites are equivalent in the restoration of the native rigid tertiary structure of parvalbumin upon Ca^{2+} association. To address this question the Ca^{2+}-induced refolding of both pike PA isoforms at 20°C [corresponds to the maximal content of α-PA secondary structure, see Fig. 3(a)] was monitored by specific heat capacity changes as measured by DSC (see Fig. 7). Calcium saturation causes a decrease in specific heat capacity of PA, reflecting the formation of the folded protein state. The Ca^{2+} titration curve for α isoform exhibits a bend near calcium to parvalbumin molar ratio about 1.0, implying that the binding of a single Ca^{2+} ion is sufficient for protein folding at 20°C. The binding of the second Ca^{2+} ion is accompanied with further, but less pronounced, increase in α-helical content and phenylalanine

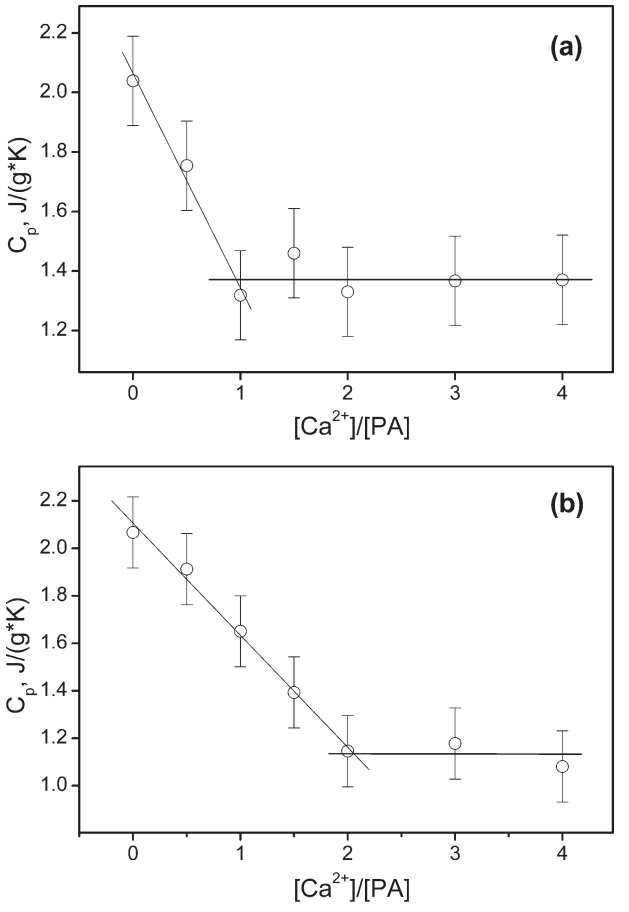

Figure 7

*Ca^{2+}-induced refolding of apo-forms of pike parvalbumin isoforms α (**a**) and β (**b**) at 20°C, as monitored by specific heat capacity changes. DSC data were obtained at heating rate 1 K/min. Buffer conditions: 20 mM glycine or 10 mM H_3BO_3, pH 9.0. K^+ was used as a counter ion in the buffer system. Apo-form of PA was prepared using the gel-filtration method described by Blum et al.[55] Concentration of PA was 1.5–2.1 mg/mL. Calcium to protein molar ratios 3 and 4 denote 1 and 10 mM concentrations of $CaCl_2$, respectively.*

fluorescence changes (data not shown). At the same time, β-PA demonstrates unexpectedly different behavior: the Ca^{2+} titration curve exhibits a bend near Ca^{2+} to PA molar ratio about 2.0 [Fig. 7(b)], which shows that both Ca^{2+} ions contribute to the folding process. This discrepancy between α and β isoforms seems to be related with the differences in the temperature dependences of their Ca^{2+} association constants (see Fig. 1). In general, enthalpy of calcium binding itself is much lower by magnitude than that for protein folding, which accompanies the metal binding in our case. For this reason the binding of Ca^{2+} ion, which results in formation of the rigid tertiary structure, should possess higher apparent enthalpy. As a result, a more prominent slope of the temperature dependence of the apparent Ca^{2+}-binding constant should be observed. Examination of Figure 1(a) shows that the binding of the first Ca^{2+} ion by α-PA is accompanied with much higher apparent enthalpy than that for the association of the second cation. This suggests that the binding of only the first calcium ion gives the major contribution to the folding process, which is in line with the DSC data [Fig. 7(a)]. Similarly, the binding of both Ca^{2+} ions to β-PA is characterized by equally high effective enthalpies [Fig. 1(b)], which suggests participation of each of the cations in the protein folding. The later conclusion may imply that the formation of the native tertiary structure in β-PA is not a single two-state process but includes formation of an intermediate. Although pike parvalbumin is a relatively small (11.5 kDa) protein, manifestation of thermodynamic domains within PA should not be excluded.

CONCLUSIONS

The presented study of genuine metal-free form of pike PA revealed a behavior drastically different from that reported for this and other representatives of parvalbumin family. Apo-parvalbumin demonstrates the absence of a fixed tertiary structure and thus belongs to the family of intrinsically disordered proteins. The quite complicated thermal denaturation behavior of PA was not observed earlier. Our preliminary experimental studies confirm that similar behavior is characteristic for some other parvalbumins. Thus, the example of parvalbumin shows that special precautions should be undertaken in order to ensure adequate studies of apo-forms of proteins, possessing extremely high affinity to calcium ions and, as a consequence, able to bind interfering sodium and, to a lesser extent, potassium ions. The later circumstance implies that under conditions resembling those *in vivo* they will be loaded by both divalent (Ca^{2+} and Mg^{2+}) and monovalent (Na^{+} and K^{+}) ions. In this sense apo-forms of these proteins do not have any evident physiological importance. Nevertheless, one could anticipate that the discovered feature of parvalbumin to be disordered in apo-state could appear under certain physiological conditions. For instance, there are examples of parvalbumin-containing vertebrate tissues and cells that accumulate urea to high concentrations.[93] Examples include marine elasmobranch fishes that accumulate urea to concentrations as high as 300–500 mmol/L as a part of the accommodation to saline environment.[93–95] Urea can also reach levels greater than 1000·mmol/L in the inner medullary region of the kidney of some dehydration tolerant mammals.[96] Urea is frequently used as a strong denaturing agent, as at high concentrations it is known to have deleterious effects on protein structure and function. These relatively high urea concentrations in those species/tissues might significantly affect the structure and conformational stability of the corresponding metal-loaded PAs, leading to the removal of metal ions and therefore allowing these proteins to behave as IDPs even under the natural conditions.

REFERENCES

1. Romero P, Obradovic Z, Kissinger CR, Villafranca JE, Garner E, Guilliot S, Dunker AK. Thousands of proteins likely to have long disordered regions. Pac Symp Biocomput 1998;3:437–448.
2. Wright PE, Dyson HJ. Intrinsically unstructured proteins: re-assessing the protein structure-function paradigm. J Mol Biol 1999;293: 321–331.
3. Uversky VN, Gillespie JR, Fink AL. Why are "natively unfolded" proteins unstructured under physiologic conditions? Proteins 2000;41:415–427.
4. Dunker AK, Lawson JD, Brown CJ, Williams RM, Romero P, Oh JS, Oldfield CJ, Campen AM, Ratliff CM, Hipps KW, Ausio J, Nissen MS, Reeves R, Kang C, Kissinger CR, Bailey RW, Griswold MD, Chiu W, Garner EC, Obradovic Z. Intrinsically disordered protein. J Mol Graph Model 2001;19:26–59.
5. Dunker AK, Brown CJ, Lawson JD, Iakoucheva LM, Obradovic Z. Intrinsic disorder and protein function. Biochemistry 2002;41:6573–6582.
6. Tompa P. Intrinsically unstructured proteins. Trends Biochem Sci 2002;27:527–533.
7. Uversky VN. Natively unfolded proteins: a point where biology waits for physics. Protein Sci 2002;11:739–756.
8. Uversky VN. What does it mean to be natively unfolded? Eur J Biochem 2002;269:2–12.
9. Uversky VN. Protein folding revisited. A polypeptide chain at the folding-misfolding-nonfolding cross-roads: which way to go? Cell Mol Life Sci 2003;60:1852–1871.
10. Radivojac P, Iakoucheva LM, Oldfield CJ, Obradovic Z, Uversky VN, Dunker AK. Intrinsic disorder and functional proteomics. Biophys J 2007;92:1439–1456.
11. Dunker AK, Obradovic Z. The protein trinity—linking function and disorder. Nat Biotechnol 2001;19:805–806.
12. Daughdrill GW, Pielak GJ, Uversky VN, Cortese MS, Dunker AK. Natively disordered proteins. In: Buchner JKT, editor. Protein folding handbook, Vol. 1. Weinheim, Germany: Wiley-VCH; 2005. pp 275–357.
13. Dunker AK, Obradovic Z, Romero P, Garner EC, Brown CJ. Intrinsic protein disorder in complete genomes. Genome Inform Ser Workshop Genome Inform 2000;11:161–171.
14. Ward JJ, Sodhi JS, McGuffin LJ, Buxton BF, Jones DT. Prediction and functional analysis of native disorder in proteins from the three kingdoms of life. J Mol Biol 2004;337:635–645.

15. Oldfield CJ, Cheng Y, Cortese MS, Brown CJ, Uversky VN, Dunker AK. Comparing and combining predictors of mostly disordered proteins. Biochemistry 2005;44:1989–2000.
16. Iakoucheva LM, Brown CJ, Lawson JD, Obradovic Z, Dunker AK. Intrinsic disorder in cell-signaling and cancer-associated proteins. J Mol Biol 2002;323:573–584.
17. Xie H, Vucetic S, Iakoucheva LM, Oldfield CJ, Dunker AK, Obradovic Z, Uversky VN. Functional anthology of intrinsic disorder. 3. Ligands, post-translational modifications, and diseases associated with intrinsically disordered proteins. J Proteome Res 2007;6:1917–1932.
18. Xie H, Vucetic S, Iakoucheva LM, Oldfield CJ, Dunker AK, Uversky VN, Obradovic Z. Functional anthology of intrinsic disorder. 1. Biological processes and functions of proteins with long disordered regions. J Proteome Res 2007;6:1882–1898.
19. Vucetic S, Xie H, Iakoucheva LM, Oldfield CJ, Dunker AK, Obradovic Z, Uversky VN. Functional anthology of intrinsic disorder. 2. Cellular components, domains, technical terms, developmental processes, and coding sequence diversities correlated with long disordered regions. J Proteome Res 2007;6:1899–1916.
20. Fuxreiter M, Simon I, Friedrich P, Tompa P. Preformed structural elements feature in partner recognition by intrinsically unstructured proteins. J Mol Biol 2004;338:1015–1026.
21. Henrotte JG. A crystalline constituent from myogen of carp muscles. Nature 1952;169:968–969.
22. Hamoir G, Konosu S. Carp myogens of white and red muscles. General composition and isolation of low-molecular-weight components of abnormal amino acid composition. Biochem J 1965;96:85–97.
23. Konosu S, Hamoir G, Pechere JF. Carp myogens of white and red muscles. Properties and amino acid composition of the main low-molecular-weight components of white muscle. Biochem J 1965;96: 98–112.
24. Pechere JF. Muscular parvalbumins as homologous proteins. Comp Biochem Physiol 1968;24:289–295.
25. Hulo N, Bairoch A, Bulliard V, Cerutti L, De Castro E, Langendijk-Genevaux PS, Pagni M, Sigrist CJ The PROSITE database. Nucleic Acids Res 2006;34:D227–D230.
26. Berchtold MW. Structure and expression of genes encoding the three-domain Ca^{2+}-binding proteins parvalbumin and oncomodulin. Biochim Biophys Acta 1989;1009:201–215.
27. Pauls TL, Cox JA, Berchtold MW. The Ca^{2+}-binding proteins parvalbumin and oncomodulin and their genes: new structural and functional findings. Biochim Biophys Acta 1996;1306:39–54.
28. Berchtold MW, Brinkmeier H, Muntener M. Calcium ion in skeletal muscle: its crucial role for muscle function, plasticity, and disease. Physiol Rev 2000;80:1215–1265.
29. Permyakov EA. Parvalbumin. New York: Nova Science Publishers; 2007.
30. Heizmann CW, Berchtold MW, Rowlerson AM. Correlation of parvalbumin concentration with relaxation speed in mammalian muscles. Proc Natl Acad Sci USA 1982;79:7243–7247.
31. Berchtold MW, Means AR. The Ca^{2+}-binding protein parvalbumin: molecular cloning and developmental regulation of mRNA abundance. Proc Natl Acad Sci USA 1985;82:1414–1418.
32. Muntener M, Kaser L, Weber J, Berchtold MW. Increase of skeletal muscle relaxation speed by direct injection of parvalbumin cDNA. Proc Natl Acad Sci USA 1995;92:6504–6508.
33. Schwaller B, Dick J, Dhoot G, Carroll S, Vrbova G, Nicotera P, Pette D, Wyss A, Bluethmann H, Hunziker W, Celio MR. Prolonged contraction-relaxation cycle of fast-twitch muscles in parvalbumin knockout mice. Am J Physiol 1999;276(2, Part 1):C395–C403.
34. Heizmann CW. Calcium signaling in the brain. Acta Neurobiol Exp (Wars) 1993;53:15–23.
35. Permyakov EA. Parvalbumin. New York: Nova Science Publishers; 2006.
36. Closset JI, Gerday C. Parvalbumins of white muscles of Gadidae–II. Properties and existence of two evolutionary lineages. Comp Biochem Physiol B 1976;55:537–542.
37. Goodman M, Pechere JF. The evolution of muscular parvalbumins investigated by the maximum parsimony method. J Mol Evol 1977;9:131–158.
38. Moncrief ND, Kretsinger RH, Goodman M. Evolution of EF-hand calcium-modulated proteins. I. Relationships based on amino acid sequences J Mol Evol 1990;30:522–562.
39. Kretsinger RH. Structure and evolution of calcium-modulated proteins. CRC Crit Rev Biochem 1980;8:119–174.
40. Nockolds CE, Kretsinger RH, Coffee CJ, Bradshaw RA. Structure of a calcium-binding carp myogen. Proc Natl Acad Sci USA 1972; 69:581–584.
41. Kretsinger RH, Nockolds CE. Carp muscle calcium-binding protein. II. Structure determination and general description J Biol Chem 1973;248:3313–3326.
42. Moews PC, Kretsinger RH. Refinement of the structure of carp muscle calcium-binding parvalbumin by model building and difference Fourier analysis. J Mol Biol 1975;91:201–225.
43. Frankenne F, Joassin L, Gerday C. The amino acid sequence of the pike (*Esox lucius*) parvalbumin 3. FEBS Lett 1973;35:145–147.
44. Gerday C. The primary structure of the parvalbumin II of pike (*Esox lucius*). Eur J Biochem 1976;70:305–318.
45. Declercq JP, Tinant B, Parello J. X-ray structure of a new crystal form of pike 4.10 beta parvalbumin. Acta Crystallogr D Biol Crystallogr 1996;52 (Part 1):165–169.
46. Declercq JP, Tinant B, Parello J, Etienne G, Huber R. Crystal structure determination and refinement of pike 4.10 parvalbumin (minor component from *Esox lucius*). J Mol Biol 1988;202:349–353.
47. Declercq JP, Tinant B, Parello J, Rambaud J. Ionic interactions with parvalbumins. Crystal structure determination of pike 4.10 parvalbumin in four different ionic environments. J Mol Biol 1991;220: 1017–1039.
48. Padilla A, Cave A, Parello J. Two-dimensional 1H nuclear magnetic resonance study of pike pI 5.0 parvalbumin (*Esox lucius*). Sequential resonance assignments and folding of the polypeptide chain. J Mol Biol 1988;204:995–1017.
49. Permyakov EA, Medvedkin VN, Kalinichenko LP, Burstein EA. Comparative study of physiochemical properties of two pike parvalbumins by means of their intrinsic tyrosyl and phenylalanyl fluorescence. Arch Biochem Biophys 1983;227:9–20.
50. Eberspach I, Strassburger W, Glatter U, Gerday C, Wollmer A. Interaction of parvalbumin of pike II with calcium and terbium ions. Biochim Biophys Acta 1988;952:67–76.
51. Permyakov EA, Kreimer DI, Kalinichenko LP, Shnyrov VL. Interactions of calcium binding proteins, parvalbumin and alpha-lactalbumin, with dipalmitoylphosphatidylcholine vesicles. Gen Physiol Biophys 1988;7:95–107.
52. Rao KS, Gerday C. Low molecular weight proteins of pike (*Esox lucius*) white muscles. I. Extraction and purification-polymorphism. Comp Biochem Physiol B 1973;44:931–937.
53. Haiech J, Derancourt J, Pechere JF, Demaille JG. A new large-scale purification procedure for muscular parvalbumins. Biochimie 1979; 61:583–587.
54. Rao KS, Gerday C. Low molecular weight proteins of pike (*Esox lucius*) white muscles. II. Chemical and physical properties. Comp Biochem Physiol B 1973;44:1113–1125.
55. Blum HE, Lehky P, Kohler L, Stein EA, Fischer EH. Comparative properties of vertebrate parvalbumins. J Biol Chem 1977;252:2834–2838.
56. Privalov PL, Potekhin SA. Scanning microcalorimetry in studying temperature-induced changes in proteins. Methods Enzymol 1986; 131:4–51.
57. Hackel M, Hinz HJ, Hedwig GR. A new set of peptide-based group heat capacities for use in protein stability calculations. J Mol Biol 1999;291:197–213.
58. Hackel M, Hinz HJ, Hedwig GR. Partial molar volumes of proteins: amino acid side-chain contributions derived from the partial molar volumes of some tripeptides over the temperature range 10-90 degrees C. Biophys Chem 1999;82:35–50.

59. Sreerama N, Venyaminov SY, Woody RW. Estimation of protein secondary structure from circular dichroism spectra: inclusion of denatured proteins with native proteins in the analysis. Anal Biochem 2000;287:243–251.
60. Kawahara K, Tanford C. Viscosity and density of aqueous solutions of urea and guanidine hydrochloride. J Biol Chem 1966;241:3228–3232.
61. Schwarzenbach G, Flaschka H. Die komplexometrische titration. Stuttgart: Ferdinand Enke Verlag; 1965.
62. Marquardt DW. An algorithm for least-squares estimation of nonlinear parameters. J Soc Ind Appl Math 1963;11:431–441.
63. Honig B, Sharp KA, Yang AS. Macroscopic models of aqueous solutions: biological and chemical applications. J Phys Chem 1993;97: 1101–1109.
64. Peng K, Vucetic S, Radivojac P, Brown CJ, Dunker AK, Obradovic Z. Optimizing long intrinsic disorder predictors with protein evolutionary information. J Bioinform Comput Biol 2005;3:35–60.
65. Obradovic Z, Peng K, Vucetic S, Radivojac P, Dunker AK. Exploiting heterogeneous sequence properties improves prediction of protein disorder. Proteins 2005;61(Suppl 7):176–182.
66. Altschul SF, Madden TL, Schaffer AA, Zhang J, Zhang Z, Miller W, Lipman DJ. Gapped BLAST and PSI-BLAST: a new generation of protein database search programs. Nucleic Acids Res 1997;25:3389–3402.
67. Rost B, Sander C, Schneider R. PHD—an automatic mail server for protein secondary structure prediction. Comput Appl Biosci 1994; 10:53–60.
68. Jones DT, Ward JJ. Prediction of disordered regions in proteins from position specific score matrices. Proteins 2003;53(Suppl 6): 573–578.
69. Williams TC, Corson DC, McCubbin WD, Oikawa K, Kay CM, Sykes BD. 1H NMR spectroscopic studies of calcium-binding proteins. 2. Histidine microenvironments in alpha- and beta-parvalbumins as determined by protonation and laser photochemically induced dynamic nuclear polarization effects. Biochemistry 1986;25: 1826–1834.
70. Permyakov EA, Kalinichenko LP, Medvedkin VN, Burstein EA, Gerday C. Sodium and potassium binding to parvalbumins measured by means of intrinsic protein fluorescence. Biochim Biophys Acta 1983;749:185–191.
71. Privalov PL, Dragan AI Microcalorimetry of biological macromolecules. Biophys Chem 2007;126:16–24.
72. Henzl MT, Hapak RC, Likos JJ. Interconversion of the ligand arrays in the CD and EF sites of oncomodulin. Influence on Ca^{2+}-binding affinity. Biochemistry 1998;37:9101–9111.
73. Henzl MT, Graham JS. Conformational stabilities of the rat alpha- and beta-parvalbumins. FEBS Lett 1999;442:241–245.
74. Agah S, Larson JD, Henzl MT. Impact of proline residues on parvalbumin stability. Biochemistry 2003;42:10886–10895.
75. Henzl MT, Agah S, Larson JD. Rat alpha- and beta-parvalbumins: comparison of their pentacarboxylate and site-interconversion variants. Biochemistry 2004;43:9307–9319.
76. Williams TC, Corson DC, Oikawa K, McCubbin WD, Kay CM, Sykes BD. 1H NMR spectroscopic studies of calcium-binding proteins. 3. Solution conformations of rat apo-alpha-parvalbumin and metal-bound rat alpha-parvalbumin. Biochemistry 1986;25:1835–1846.
77. Filimonov VV, Pfeil W, Tsalkova TN, Privalov PL. Thermodynamic investigations of proteins. IV. Calcium binding protein parvalbumin. Biophys Chem 1978;8:117–122.
78. Landau LD, Lifshitz LP. Statistical physics, Part 1. Oxford: Pergamon Press; 1980.
79. Griko YV, Privalov PL. Thermodynamic puzzle of apomyoglobin unfolding. J Mol Biol 1994;235:1318–1325.
80. Wilson G, Hecht L, Barron LD. The native-like tertiary fold in molten globule alpha-lactalbumin appears to be controlled by a continuous phase transition. J Mol Biol 1996;261:341–347.
81. Burstein EA. Mol Biol (Mosk) 1971;5:214–225.
82. Burstein EA. Intrinsic protein fluorescence: origin and applications. Moscow: VINITI; 1977.
83. Permyakov EA. Luminescent Spectroscopy of Proteins. Boca Raton, Ann Arbor, London, Tokyo: CRC Press, Inc.; 1993.
84. Kuznetsova IM, Turoverov KK, Uversky VN. Use of the phase diagram method to analyze the protein unfolding-refolding reactions: fishing out the "invisible" intermediates. J Proteome Res 2004;3: 485–494.
85. Closset J, Gerday C. Conformational studies on parvalbumins by circular dichroism. Biochim Biophys Acta 1975;405:228–235.
86. Maximov EE, Mitin YV. Binding of calcium by fragment 38-108 of pike parvalbumin. Biochimie 1979;61:751–754.
87. Dolgikh DA, Gilmanshin RI, Brazhnikov EV, Bychkova VE, Semisotnov GV, Venyaminov SY, Ptitsyn OB. Alpha-lactalbumin: compact state with fluctuating tertiary structure? FEBS Lett 1981;136: 311–315.
88. Kuwajima K. The molten globule state as a clue for understanding the folding and cooperativity of globular-protein structure. Proteins 1989;6:87–103.
89. Finkelstein AV, Shakhnovich EI. Theory of cooperative transitions in protein molecules. II. Phase diagram for a protein molecule in solution. Biopolymers 1989;28:1681–1694.
90. Mayor U, Grossmann JG, Foster NW, Freund SM, Fersht AR. The denatured state of Engrailed homeodomain under denaturing and native conditions. J Mol Biol 2003;333:977–991.
91. Obradovic Z, Peng K, Vucetic S, Radivojac P, Dunker AK. Exploiting heterogeneous sequence properties improves prediction of protein disorder. Proteins 2005;61(Suppl 7):176–182.
92. Gosselin-Rey C, Bernard N, Gerday C. Conformation and immunochemistry of parvalbumin 3 from pike white muscle. Modification of the arginine residue with 1,2-cyclohexanedione. Biochim Biophys Acta 1973;303:90–104.
93. Yancey PH. Compatible and counteracting solutes. In: Strange K, editor. Cellular and molecular physiology of cell volume regulation. Boca Raton: CRC Press; 1994. pp 81–109.
94. Forster RP, Goldstein L. Intracellular osmoregulatory role of amino acids and urea in marine elasmobranchs. Am J Physiol 1976;230: 925–931.
95. Treberg JR, Speers-Roesch B, Piermarini PM, Ip YK, Ballantyne JS, Driedzic WR. The accumulation of methylamine counteracting solutes in elasmobranchs with differing levels of urea: a comparison of marine and freshwater species. J Exp Biol 2006;209(Part 5):860–870.
96. Yancey PH. Osmotic effectors in kidneys of xeric and mesic rodents: corticomedullary distributions and changes with water availability. J Comp Physiol [B] 1988;158:369–380.